ATS/Note/2010/043 (MD SPS)

2010-09-28

Gianluigi.Arduini@cern.ch

UA9 SPS MD report of 30 June-1 July 2009

MD participants: O. Andujar[a], G. Arduini[a], C. Bracco[a], S. Cettour-Cave[a], G. Crockford[a], F. Follin[a], Y. Gavrikov[b], S. Gilardoni[a], V. Ippolito[a], Y. Ivanov[b], Y. LeBorgne[a], E. Laface[a], R. Losito[a], A. Masi[a], S. Massot[a], E. Métral[a], D. Mirarchi[a], L. Pereira[a], V. Previtali[a], S. Redaelli[a], W. Scandale[a], M. Silari[a], G. Smirnov[a], A. Taratin[c], E. Veyrunes[a]

[a]CERN, European Organization for Nuclear Research, Geneva, Switzerland
[b]Petersburg Nuclear Physics Institute (PNPI), Gatchina, Russia
[c]Joint Institute for Nuclear Research (JINR), Dubna, Russia

Keywords: Channeling, Crystals, SPS

Summary

This note briefly reports on the MD period dedicated to the crystal channelling experiment (UA9) installed in SPS LSS5 performed on 30 June-1 July 2009.

1. Summary of the Machine Development

Twenty-four hours (three shifts) were attributed to UA9, from 08:00 on Tuesday 30 June to 08:00 on Wednesday 1 July.

The main aims of the MD session were:

- Complete the setting-up of the beam with the required conditions for the measurement which could not be completed during the previous session because of the reduced time available and to fix some of the problems encountered during the last session (mainly timing issues);
- Verification of the operation of the beam instrumentation in coast (in particular Wire Scanners, Closed Orbit, SPS Beam Loss Monitors);
- Preliminary set-up of the excitation by means of the transverse feedback
- Setting-up of the various detectors and monitors in order to assess their suitability for the future UA9 machine study sessions;
- Validation of the procedure for the beam-based alignment of the various devices installed in the SPS LSS5 area.

2. SPS set-up

During the previous MD session some timing problems were noticed which could not be fixed during the session because they required expert intervention. In particular, the injection transfer line (TT10) magnets were pulsing even when the machine was in coast. Moreover, the magnet MDSH1198 was pulsing leading to periodic orbit distortions (every 18 s) making the alignment and measurement not possible.

The RF functions corresponding to the pulsed cycle (including acceleration) were executed in coast instead of the coast ones. For that reason the RF voltage during the acceleration from 26 to 120 GeV/c had to be kept constant in order to have a constant voltage during the coast.

Both the above problems were fixed in advance of the Machine Development session and did not appear during the session.

The problems observed with the interlocks in the previous session were solved in advance of the test.

The sequence of actions to go in coast is listed below (see references in [1][2]):

1) Pulse stop on the Main power supply with the sequencer.

2) Load with the sequence manager the sequence.

   Name: LHC2-0/1/2 (Coastable 120 GeV);

   Description: LHC2 Beam with LHCINDIV, coastable120 GeV (UA9);

3) Pulse Start on the Main power supply with the sequencer.

4) Change the accelerator mode:

   a. FTARGET => NO EXTRACTION;

   b. CNGS => NO EXTRACTION;

   c. LHC-B1 => NO EXTRACTION;

   d. LHC-B2 => NO EXTRACTION.

5) Set all equipment so to eliminate all the SW interlocks, in particular

   a. Switch OFF the extraction bumpers;

   b. Retract the LSS2, LSS4, LSS6 extraction girders;

   c. Extraction kickers LSS4 and LSS6 in Stand-by;

   d. Set the high voltage to 0V for the LSS2 Electrostatic Septa. Do not switch them off.

6) Mask the following Software interlocks:

   a. MKD EARLY ENABLED;

   b. MKD EARLY LHC VETO;

c. TT10 POWER CONVERTERS (if you want to stop TT10 some power converters when you are in coast);

d. BLRING DUMP CHANNEL VETO;

e. UA9 LSS5.

7) Mask input 8 on the BIC BA5 and the survey of the mask status on SIS before using the collimators

8) Switch ON the MKP (4 generators) for the timing user LHC2 and COASTPR1 and with the same settings as for LHC2 user.

Frequent trips of the SMQ (main quadrupole) power converter stations were observed at the time of the recovery after a coast. These were understood after the end of the machine study session and were found to be due to a timing definition problem.

The acquisition of the beam profile measurements by means of the wire scanner BWS51995, not working during the previous MD, were tested and found to work properly after a modification done to the application software. The option "Scan Now" was used. Several beam profiles could be taken during the whole machine development session.

Some tails were observed in the horizontal plane (see Fig. 1) but this was not considered to be an issue for the machine study and no attempt was done to further investigate the effect.

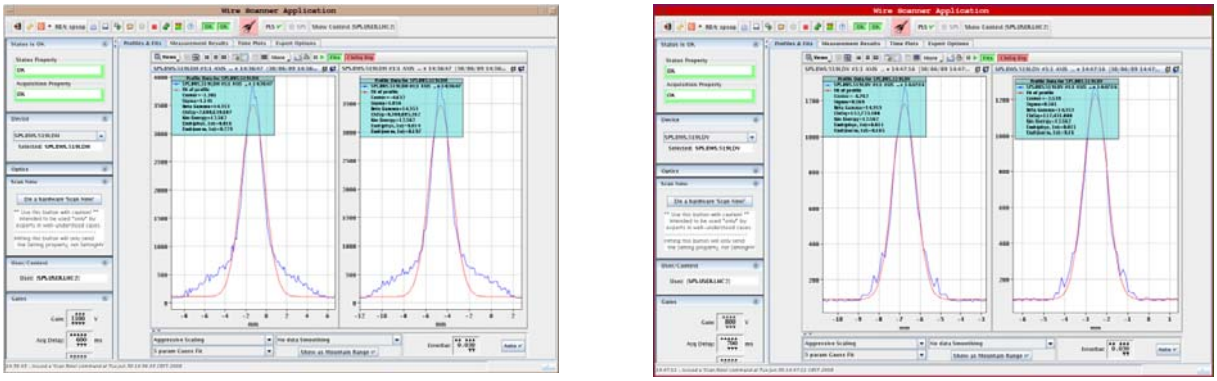

Figure 1 Horizontal (left) and vertical (right) beam size measurements performed in coast at 120 GeV/c with the wire scanner BWS51998. For each measurement two profiles are shown. They correspond to the movement of the wire scanner in one direction and then in the opposite direction to resume its parking position.

The settings of the MOPOS delays were adjusted in order to obtain acceptable beam position closed orbit measurements. The settings are reproduced in Fig. 2 below for reference.

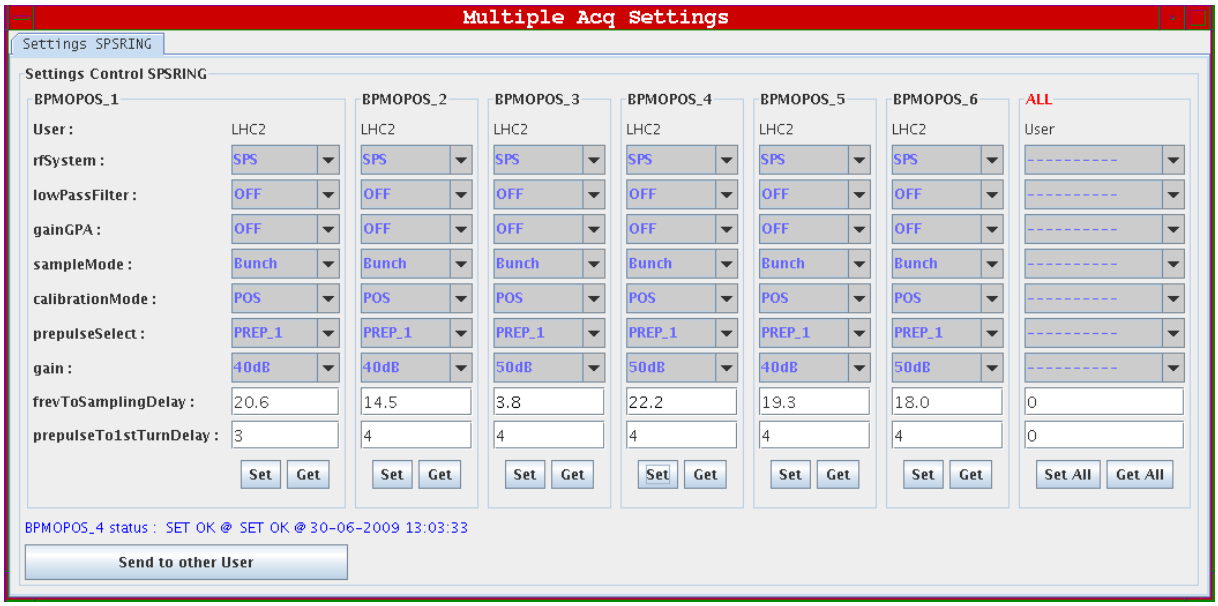

Figure 2 MOPOS settings for the orbit acquisition at the SPS.

Measurements of the orbit in coast were still not possible. The 1000 turn acquisition could not be tested thoroughly.

The beam was injected at 26 GeV/c, accelerated to 120 GeV/c and then put in coast. During the operation in pulsed mode and coast the timing table is executed repeatedly with a period of 18 s. The beam consisted of a single bunch with a population of about $4 – 5\times10^{10}$ protons (LHCINDIV) with typical transverse r.m.s. normalized emittances $\varepsilon^* = 1.9$ (H)/1.4 (V) □m (in the horizontal plane the core has been considered for the determination of the r.m.s. beam size).

The evolution of the beam population during the machine development session is shown in Fig. 3 starting from 15:00 when the recording of the intensity data has started. A signal corresponding to 50×10^8 is visible in the plot. This corresponds to a calibration pulse used for the Beam Current Transformer and triggered at every cycle.

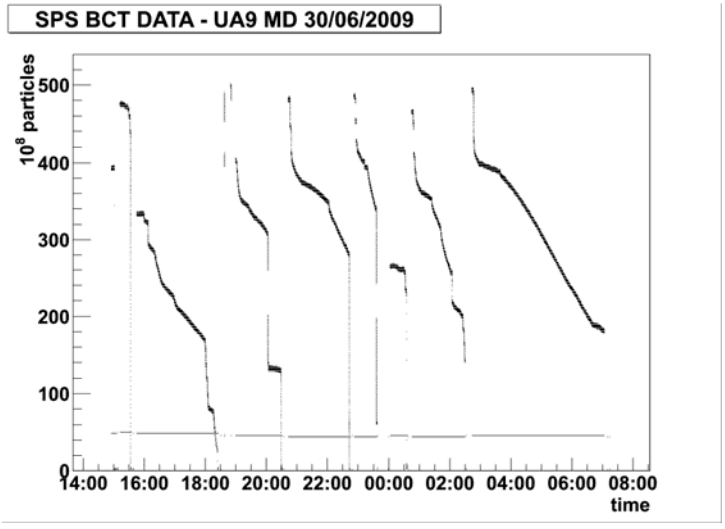

Figure 3 Evolution of the beam population during the machine development session.

The corresponding beam population reduction rate as a function of time is shown in Fig. 4**.**

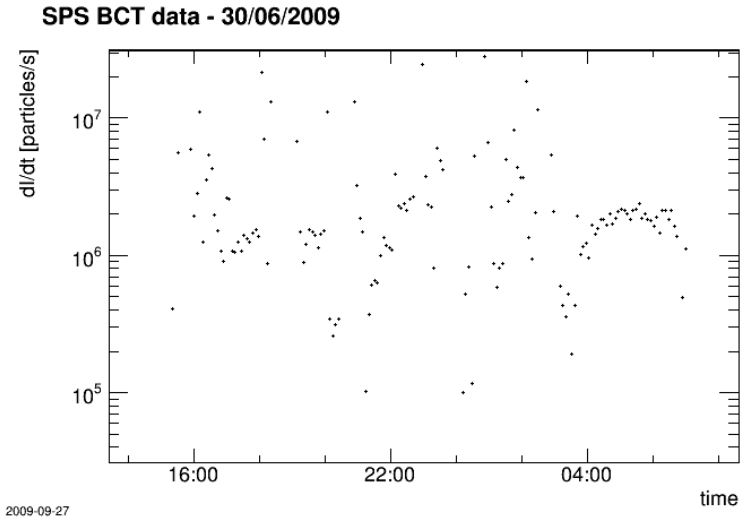

Figure 4 Evolution of the beam population reduction rate during the machine development session.

The orbit was corrected during the ramp and at high energy before putting the machine in coast so to achieve an r.m.s. value of the beam position at the SPS beam position monitors of 1.8 (H) and 2.5 (V) mm (see Fig. 5).

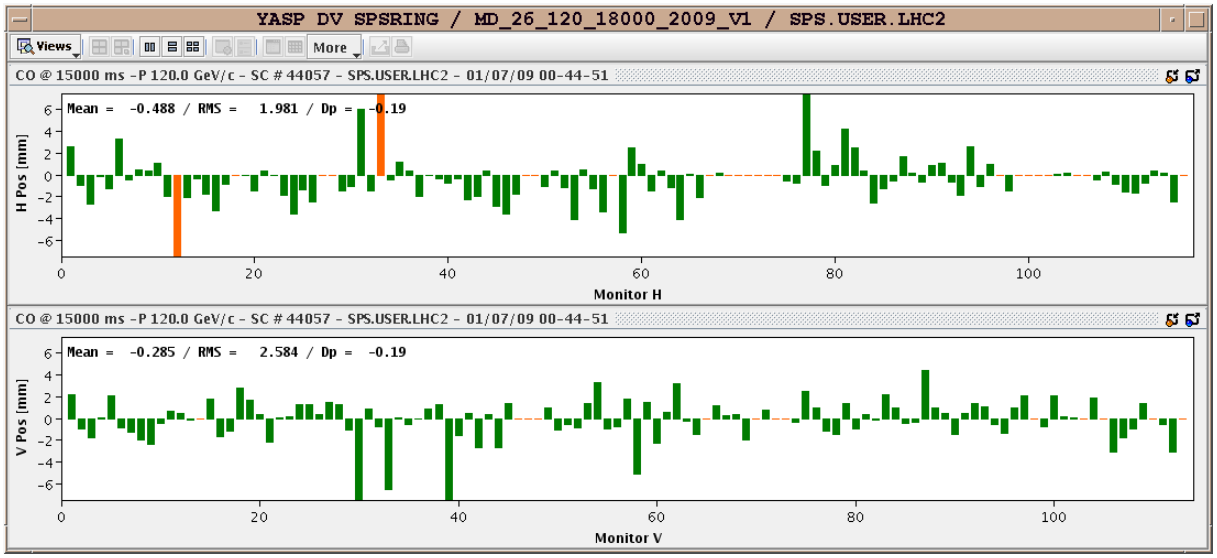

Figure 5 Orbit measurement at 120 GeV/c before going in coast.

The chromaticity was corrected to $\xi = (\Delta Q/Q)/(\Delta p/p) \sim +0.1$ in both planes and the tunes were set to ($Q_H = 26.13$ – $Q_V = 26.18$) as can be seen in Fig. 6 showing the tune evolution over 15 s taken in coast without excitation.

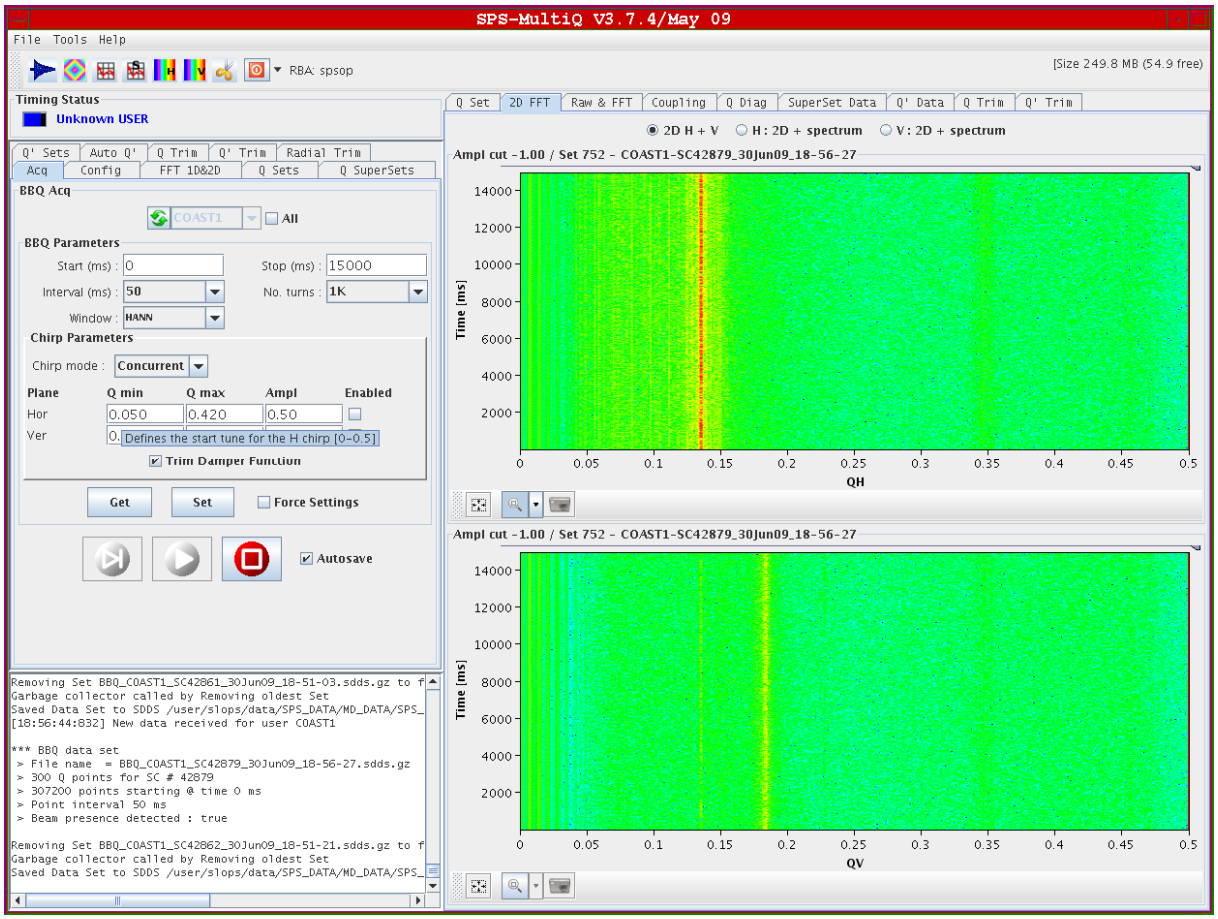

Figure 6 Tune spectra over 15 s while in coast.

A preliminary commissioning of the transverse beam excitation has been conducted with the available tools. The excitation has been applied in the horizontal plane by means of the transverse feedback. For this first session only a limited set of tools could be made available. This allowed conducting a frequency sweep with 1 kHz span around $(1 - Q_H)f_{rev} = 0.87\ f_{rev} = 37.7$ kHz and over a period of 15 s every 18 s [3]. This type of excitation resulted in a non uniform diffusion speed and in large variation of the losses vs. time and for that reason it was abandoned during the MD.

3. Description of the experimental set-up

Fig. 7 and 8 show the schematic layout of the UA9 experiment. The positions of the detectors installed for the experiment (scintillation counters – TEC and QDs –, GEM and Cherenkov detectors) and of the LHC BLM (ionization chambers and SEM) are indicated as well. Crystal 1 is a single strip Si crystal, Crystal 2 is a quasi-mosaic Si crystal, TAL is a 66 cm long tungsten absorber.

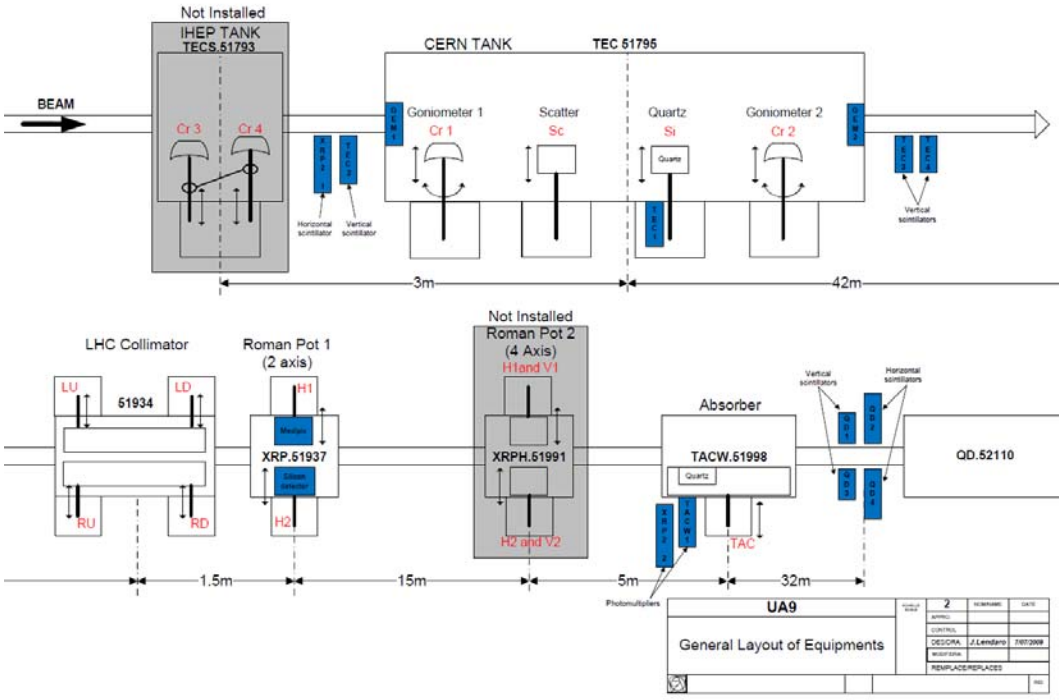

Figure 7 Schematic layout of the installation in LSS5 in the SPS for the Crystal experiment.

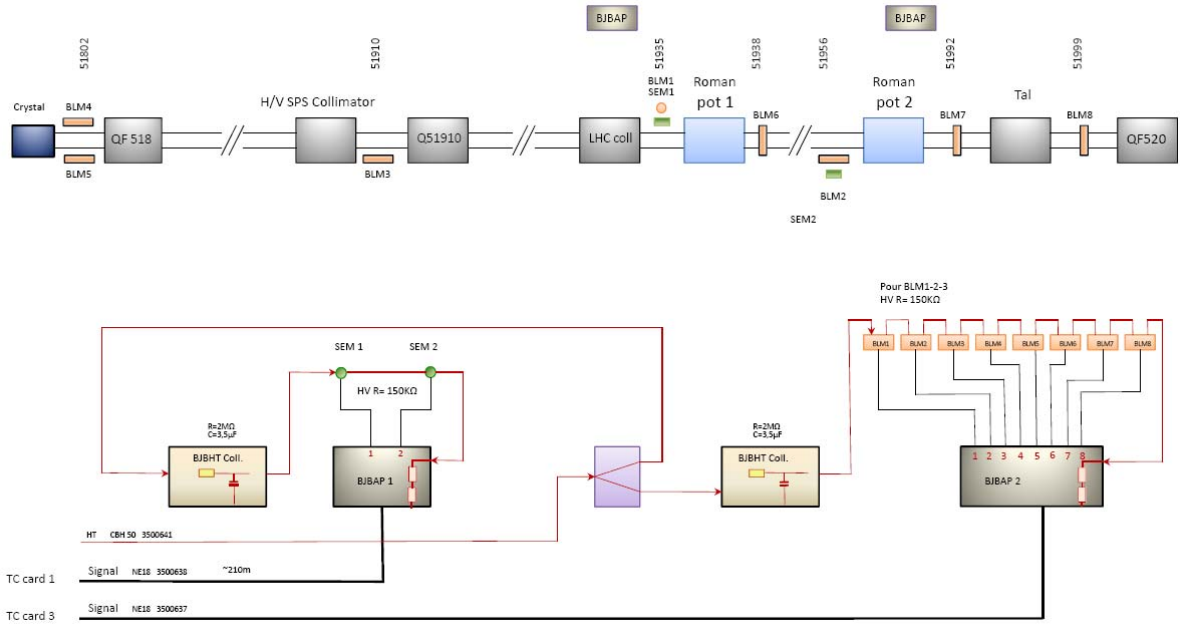

Figure 8 Schematic layout of the installation in LSS5 in the SPS for the Crystal experiment with an electrical scheme. Courtesy of E. Effinger (BE/BI).

The photos of the installation indicating the detail of the positioning of the various detectors are shown in Fig. 9 to 15.

Figure 9 BLM 1 and SEM 1: (SPS-Position: 51935) seen the outside of the machine (left) and from top (right). They are installed 170 cm downstream of the middle of the LHC collimator (TCSP.51934). Both the BLM and SEM are installed parallel to the beam pipe and centred vertically. Both monitors are mounted at a distance of 30 cm to the beam pipe wall. Courtesy of E. Effinger.

Figure 10 BLM 2 and SEM 2: (SPS-Position: 51956) seen from the inside of the machine (left) and from top (right). They are positioned 500 cm downstream of BLM6 (see below). The BLM and SEM are installed parallel to the beam pipe at a distance of 3 cm to the beam pipe wall. The SEM is centred vertically and the BLM 15 cm lower. Courtesy of E. Effinger.

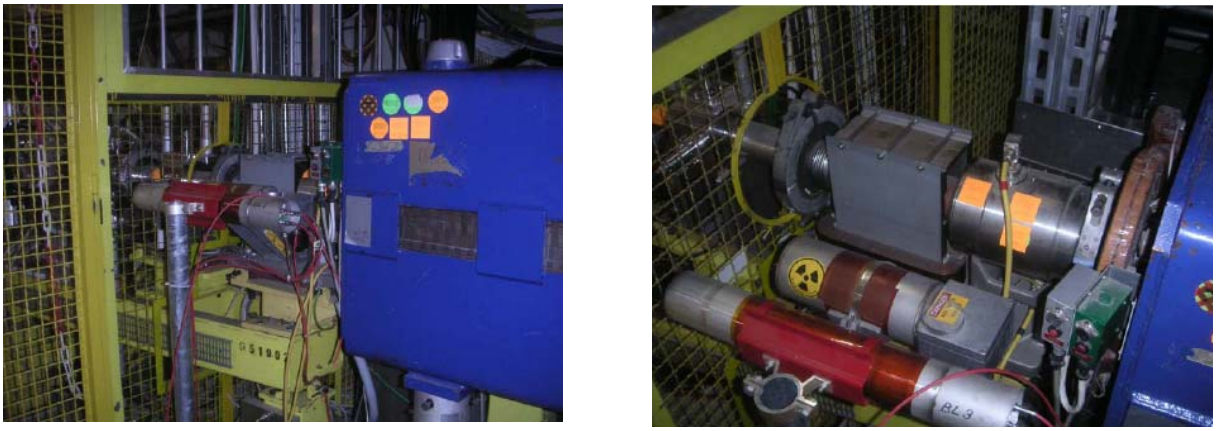

Figure 11 BLM 3: (SPS-Position: 51910) seen from the inside of the machine (left) and from top (right). It is installed close to the corrector MDV.51910 and to the corresponding SPS BLM (installed closer to the beam pipe in the picture). It is placed parallel to the beam pipe at a distance of 44 cm to the beam pipe wall. Courtesy of E. Effinger.

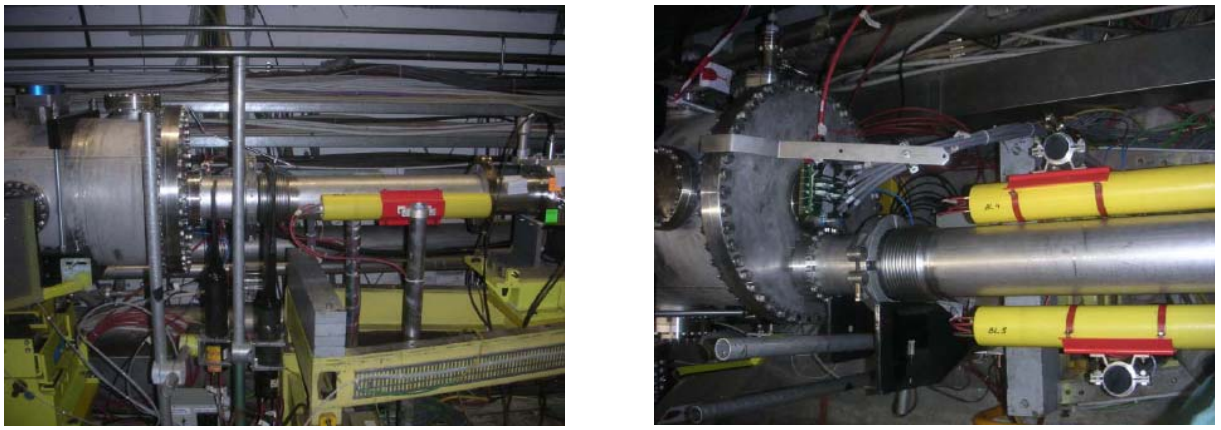

Figure 12 BLM 4 and BLM 5: (SPS-Position: 51802) seen from the inside of the machine (left) and from top (right). They are installed at a distance of 82 cm downstream of the end of the Crystal tank (TEC.51795). They are placed parallel to the beam pipe and at a distance of 1 cm (BLM 4) and 2.5 cm (BLM 5) to the beam pipe wall. Courtesy of E. Effinger.

Figure 13 BLM 6: (SPS-Position: 51938) seen from the inside of the machine (left) and from top (right) Distance: 100 cm from middle of the Roman Pot 1 to the BLM. It is placed perpendicular to the beam pipe at a distance of 2 cm to the beam pipe wall. Courtesy of E. Effinger.

Figure 14 BLM 7: (SPS-Position: 51992) seen from inside the machine (left) and from top (right). It is installed at a distance of 100 cm downstream of the middle of the Roman Pot 2 (not installed yet). It is placed perpendicular to the beam pipe at a distance of 2 cm to the beam pipe wall. Courtesy of E. Effinger.

Figure 15 BLM 8: (SPS-Position: 51999) seen from the inside of the machine (left) and from top (right) at a distance of 67 cm downstream of the middle of TAL collimator (TACW.51998). It is placed perpendicular to the beam pipe at a distance of 1 cm to the beam pipe wall. Courtesy of E. Effinger.

The structure of the data saved for the UA9 detectors and movable devices is presented in Section 9 (Appendix).

4. Alignment of movable devices, local loss monitoring and channelling detection

4.1. Angular scan

Keeping the LHC collimator as the primary collimator, the crystal was slowly inserted toward the edge of the primary beam. When the crystal touched the edge of the beam, the losses at the beam loss monitors immediately downstream of the crystal increased, showing that the crystal was at the same betatronic amplitude (in unit of beam sigma) as the collimator with respect to the beam orbit. Using the same procedure also the TAL was aligned, and then slightly retracted (6 – 7 sigma) in order not to intercept the beam directly. After the element alignment the collimator was completely opened and the angular scans of the crystal started. The first tested crystal was Crystal 2.

Fig. 16 shows the time evolution of the signals of the LHC BLMs (1, 2 and 4) located downstream of the crystal tank and of scintillation counters (TEC3 and TEC4) located downstream of the crystal tank during the angular scan of Crystal 2.

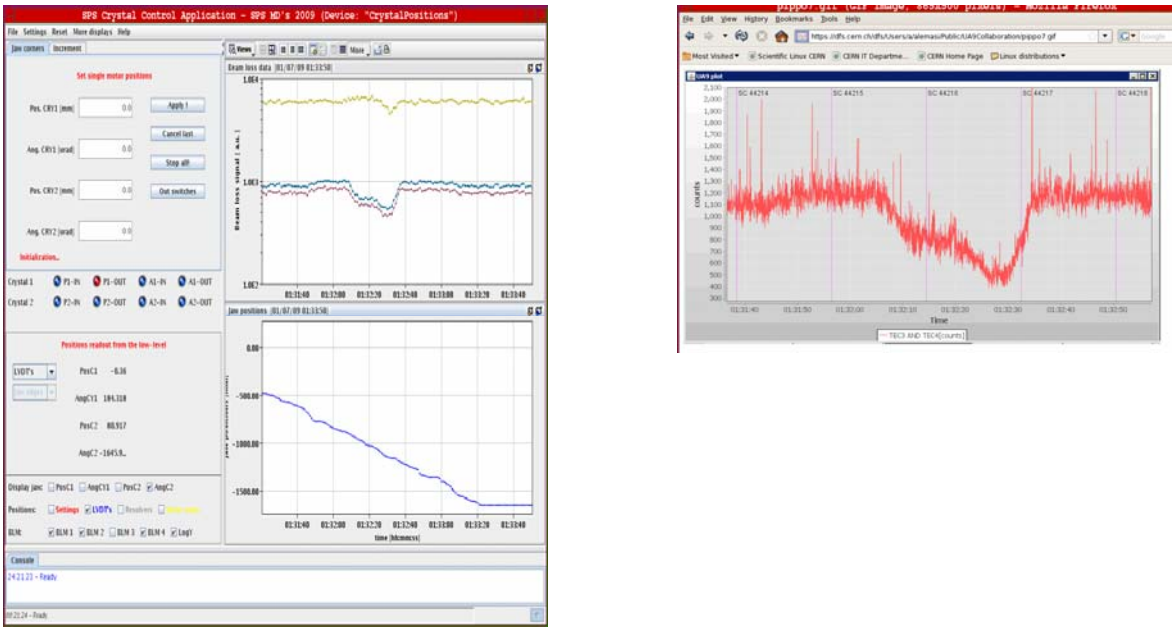

Figure 16 Time evolution of the LHC BLM (1, 2 and 4) signals (top left) and of scintillation counters (TEC3 and TEC4) signals (top right) during the angular scan (bottom left) of Crystal 2.

The result of an additional scan is shown in Fig. 17 for the BLMs 4, 5 (immediately after the crystal) and 8 (immediately after the TAL). The counting rate of the nuclear reactions in the crystal 2 shows a deep (signal from BLM 4 and 5) due to channelling, during which the rate is decreased by a factor of 3. The plateau to the right of the channeling peak is due to Volume Reflection [4] and it covers a range of about 150 μrad (as expected). No significant variation of the signal in BLM 8 is observed, which is not understood.

Crystal 2 was then retracted and Crystal 1 was then aligned. The same angular scans were repeated, the results are shown in Fig. 18. Multiple channeling-Volume Reflection regions were observed: a main peak appears at an angle of -1800 μrad, but there are other three peaks at about 0 μrad, 500 μrad and 1500 μrad.

The orientation of the Crystal 1 is close to the axis <111>. The observed behaviour could be an indication of channeling deflection by skew planes, i.e. of a tilt of the crystal as already observed in the H8 experiment. It is also interesting to consider the increased losses at BLM 8 downstream of the TAL just after the channeling peak at -1800 μrad, where the Volume Reflection (VR) region is expected. To magnify this region a new angular scan was performed with a smaller range. The result of this new scan is presented in Fig. 19 again for BLMs no. 4, 5 and 8 respectively. The BLMs at the crystal (BLM 4 and 5) show a clear channeling peak at -1800 μrad, and then a plateau up to about -1600 μrad, which is compatible with the volume reflection. The losses at the TAL (BLM 8) decrease abruptly in the channeling region, while they increase in the VR region. This behaviour is not understood and it could be an indication that the channeled beam is intercepted in a different position in the machine and not at the TAL. This hypothesis should be confirmed in next MDs using the SPS BLMs.

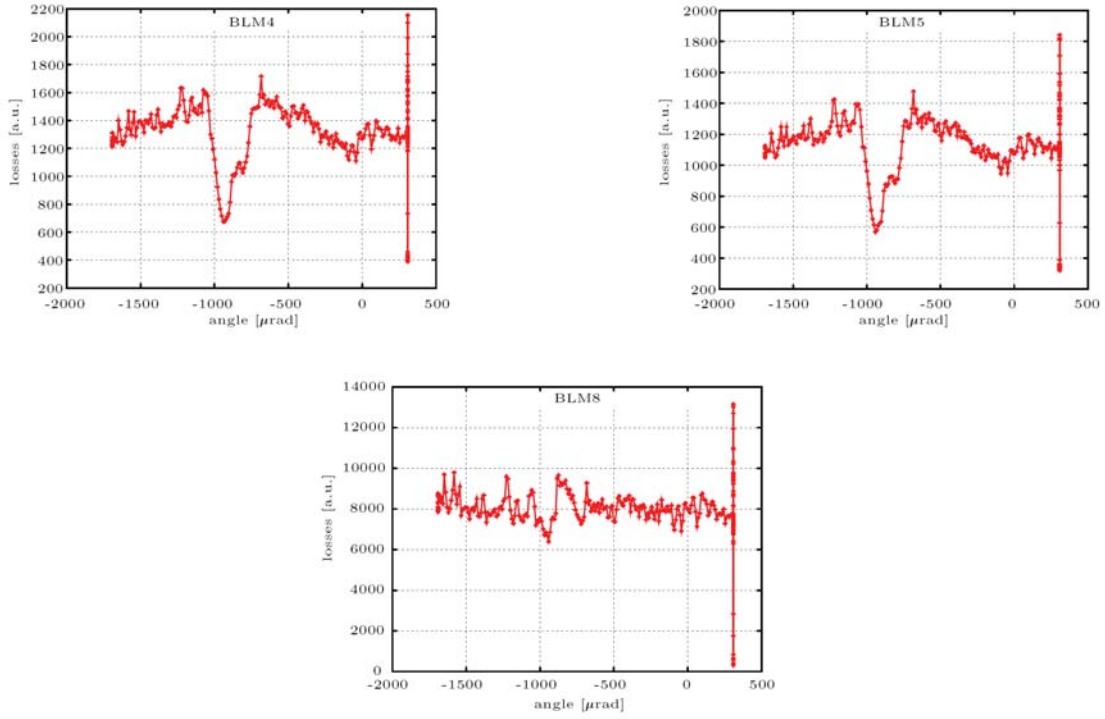

Figure 17 Crystal 2 angular scan: signal on BLM 4, 5 and 8. The counting rate of the nuclear reactions in the crystal 2 shows a deep due to channelling, during which the rate is decreased by a factor of 3. The plateau to the left of the channeling peak is due to the volume reflection and covers a range of about 150 μrad (as expected).

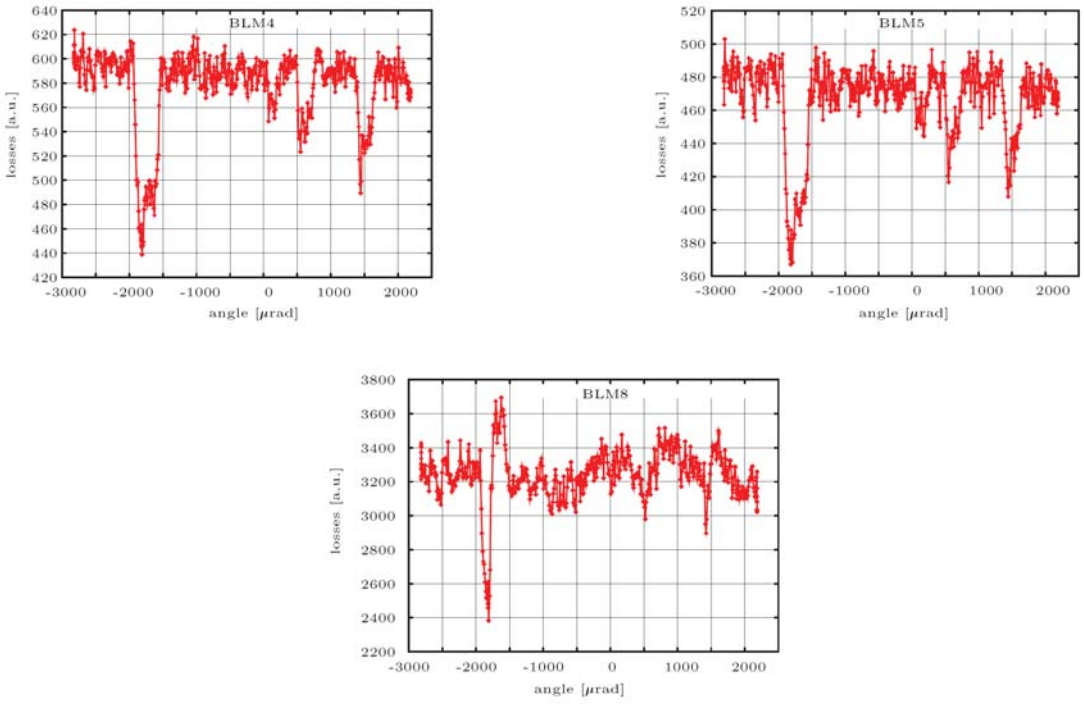

Figure 18 Crystal 1 angular scan: signals from BLM 4, 5 and 8.

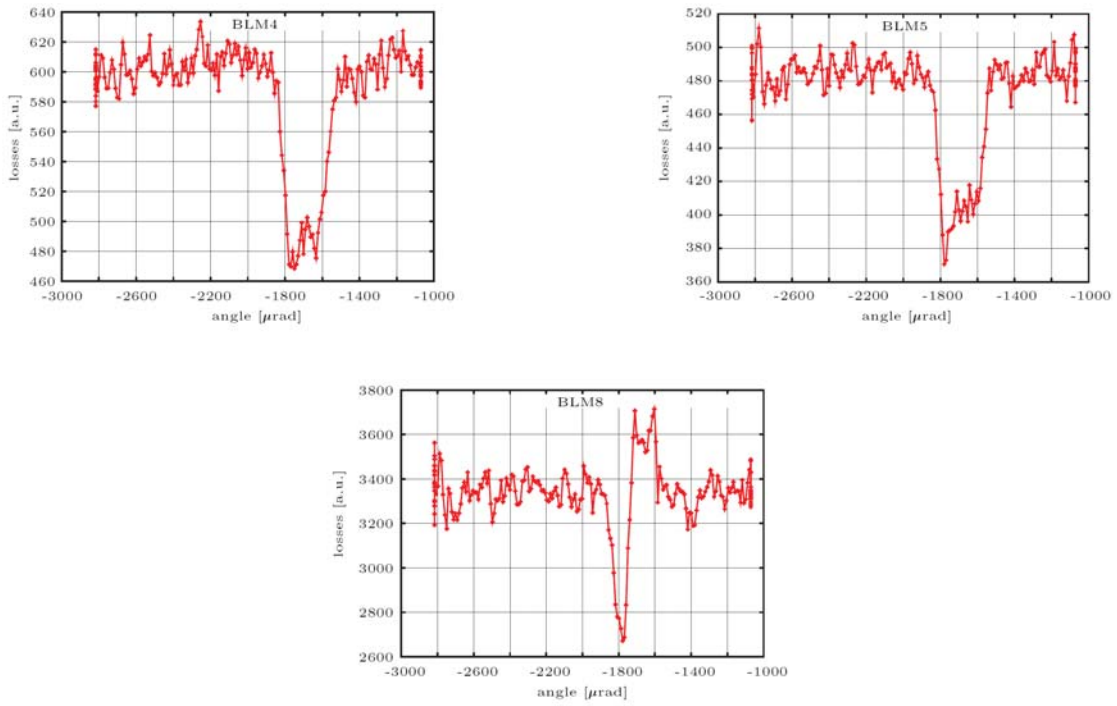

Figure 19 Crystal 1 refined angular scan: signals from BLM 4, 5 and 8.

4.2. Collimator scan

After the angular scan the attention was focused on measuring the displacement of the channeled beam via a collimator scan: the goniometer is positioned at an angle corresponding to the middle of the channeling peak and the LHC collimator is slowly moved towards the beam edge, up to when it touches the primary beam. In order to see the losses at the collimator (proportional to the population of the intercepted beam) as a function of the collimator position the losses are registered with the BLM 1 and 2 (downstream of the collimator). During these scans the TAL is kept at a slightly larger amplitude than the crystal. The evolution of the losses at BLM 1 during the collimator scan is presented in Fig. 20 for the first channelling peak of Crystal 1 (–1800 μrad).

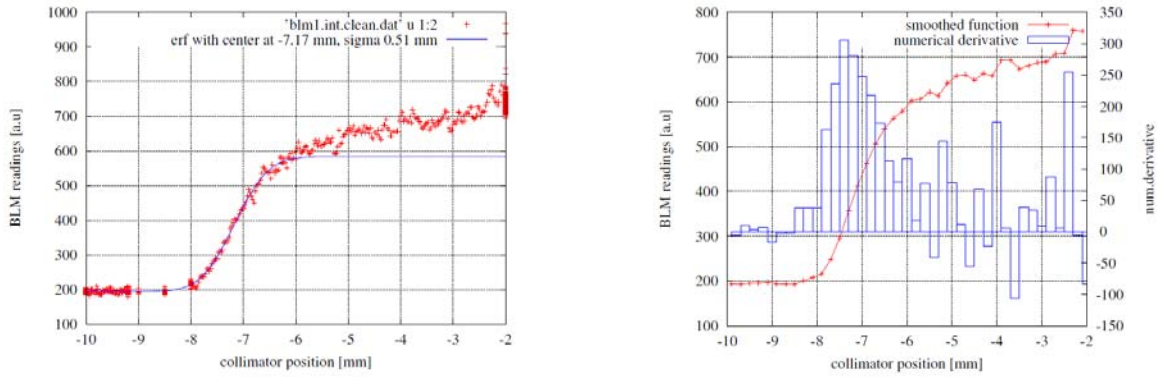

Figure 20 Crystal 1 in channeling position at –1800 μrad: BLM 1 signal evolution during the collimator scan (left) and numerical derivative of the BLM signal (right)

The loss increases from left to right as the collimator hit and destroy the channeled beam. Later the losses stabilize and show a plateau indicating that there is an area with lower particle population (clearance of about 5 mm) in between the channeled beam and the circulating beam. Continuing in the scan the losses increase again since the LHC collimator is intercepting the circulating beam. The increase of losses at BLM 1 is fitted with the error function: the centre is at –7.17 mm, and its sigma about 0.51 mm. The latter are the mean position with respect to the collimator reference system and the r.m.s. size of the channelled beam. The same scan was smoothed and a numerical derivative was computed in an attempt of reconstructing the beam profile at the collimator location. The peak is compatible with the –8 mm obtained with the error function, but the noise on the signal does not permit to have further significant information on the structure of the beam between the channeled peak and the edge of the primary beam. The noise on the signal could be due to the sum of an intrinsic noise in the BLM, the precision of collimator's position and the beam diffusion.

The scan was repeated for other angular positions of the crystal: an amorphous position (–2040 μrad), a volume reflection position (–1693 μrad), and two secondary channeling peaks, respectively at 1410 and –5010 μrad. The results of these scan are presented in Fig. 21.

When the crystal is in amorphous position (top left) the particles of the halo experience multiple scattering which is simply enhancing the beam tails. Moving the LHC-type collimator into the beam shows that the loss regime is compatible with a population of all the space around the core of the beam with no gap in the transverse distribution. The losses are quasi constant until one touches the core of the beam.

The volume reflection (top right) shows a behaviour similar to that observed in the amorphous regime, as probably the reflected protons did not intercept the collimator. It is also interesting to notice that for the other channeling peaks (bottom) the losses are lower with respect to the first channeling peak (a factor of 2 or 3), meaning that the channeling efficiency is lower.

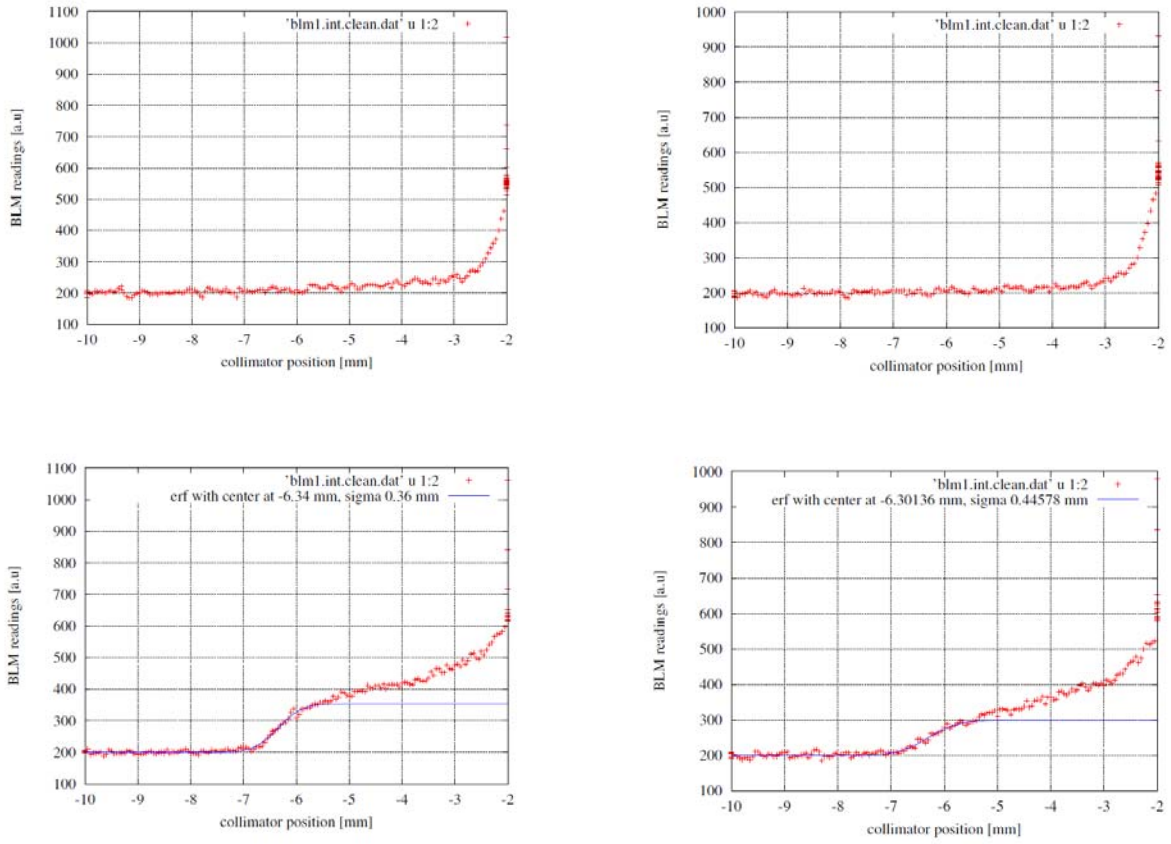

Figure 21 BLM 1 signal evolution during LHC collimator scans for: Crystal 1 in amorphous position at –2040 μrad (top left). Crystal 1 in volume reflection position at –1693 μrad (top right). Crystal 1 in channeling position at 1410 μrad (bottom left). Crystal 1 in channelling position at –5010 μrad (bottom right).

5. Beam Loss Maps

Beam loss data were taken with the SPS BLMs distributed all around the ring for three different regimes of the crystal based two-stage collimation system:

1. Crystal 2 in amorphous (i.e. misaligned with respect to the channeling position) mode with TAL IN
2. Crystal 2 in channeling mode with TAL IN
3. Crystal 2 in channeling mode with TAL OUT

In all cases the LHC collimator was retracted.

The average BLM signal for the three cases above is shown in Fig. 22 for each of the 6 SPS sextants (each containing 36 BLMs).

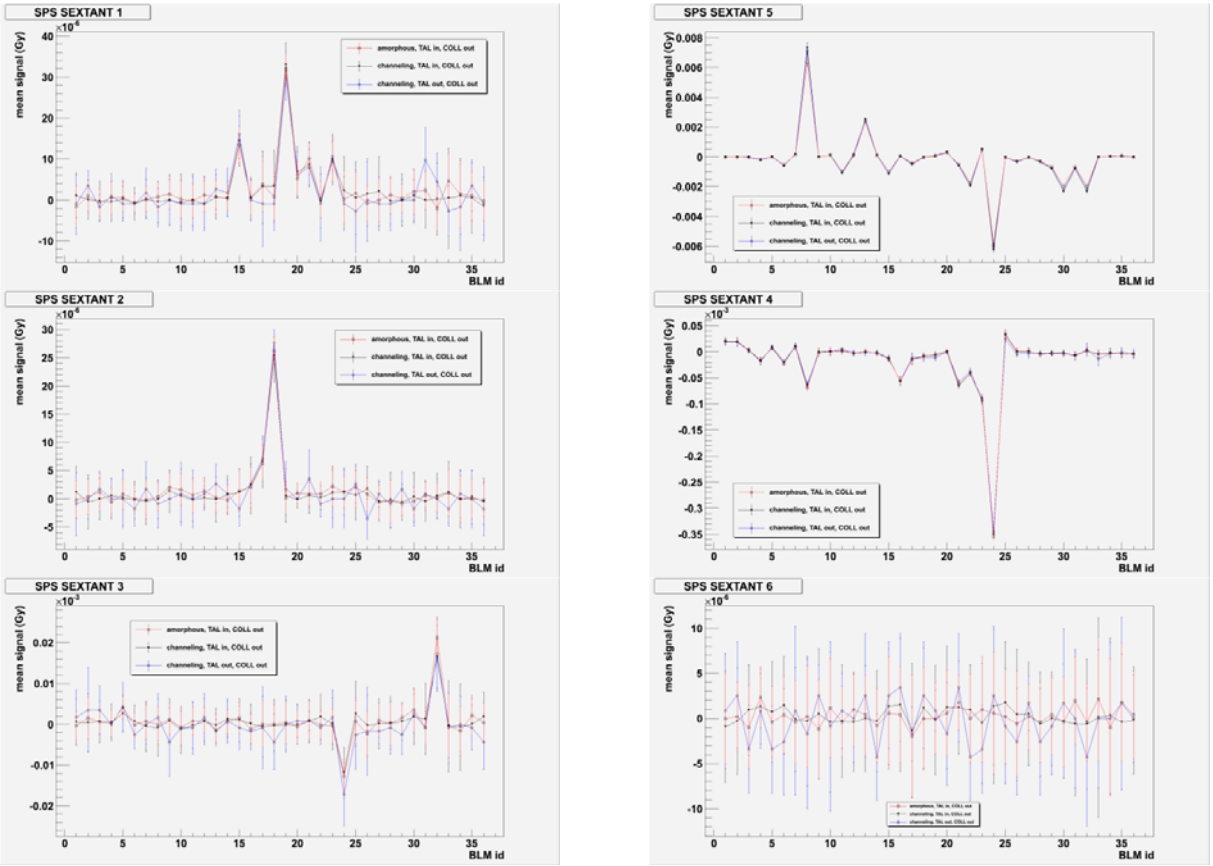

Figure 22 Average SPS BLM signal for three different modes of operation of the crystal based two-stage collimation system.

The signal to noise ratio is not sufficient to distinguish any difference in the beam loss distribution around the SPS ring for the three considered configurations.

6. Remaining issues and actions

The following issues remain to be addressed for the following sessions:

1. Timing definition leading to trip of the SMQ (Main Quadrupole) Power supplies during the recover from a coast.
2. Orbit measurement in coast not working
3. 1000 turn orbit acquisition data to be tested thoroughly and data to be analyzed
4. Transverse noise excitation
5. Insufficient signal-to-noise ratio for the beam loss measurement around the ring for the beam population and loss rate considered.
6. The wire scanner data were not saved in files

7. Acknowledgements

We would like to thank T. Bohl and U. Wehrle for the setting-up of the RF system for the Machine Development session and R. Assmann for the contribution to the preparation of the experiment and analysis of the data.

8. References

[1] Some references for the 120 GeV/c coast with protons: https://ab-mgt-md-users.web.cern.ch/ab-mgt-md-users/2009/MDCycles/SomeReferencesForpCoastAt120GeV/Ref.htm.

[2] Reports on the ELogBook: https://ab-mgt-md-users.web.cern.ch/ab-mgt-md-users/2009/MDCycles/SomeReferencesForpCoastAt120GeV/ELogBook.htm.

[3] E. Métral et al., Controlled Transverse Emittance Blow-Up in the CERN SPS, PAC09 Proceedings.

[4] A. M. Taratin and S. A. Vorobiev, Nucl. Instrum. Methods Phys. Res., Sect. B 26, 512 (1987)

9. Appendix: UA9 Detectors logging files format

The files organization and the logging data format for each UA9 detectors and motorizations are presented

9.1. Files Organization

Medipix	Data UA9 Medipix installed in the roman pot 1 H2 axis
GEM1	Data GEM 1 installed in the tank upstream Crystal 1
GEM2	Data GEM 2 installed in the tank downstream Crystal 2
Scintillation counters	Data Scintillation counters
PositionsA	Positions of Crystal1 Goniometer 1, Crystal2 Goniometer 2, Photomultiplier 1 Detector
PositionsB	Positions of Scatterer, IHEP goniometer, Roman Pot 1
PositionsC	Positions of Roman Pot 2
TAC_position	TAC position data
LSS5Collimator	Axes position of the LSS5 collimator

The files are indexed with progressive numbers to limit the size.

In each file the columns are TAB separated and array elements are COMMA separated.

The logging data of each MD are contained in the directory *MD_MDDate* at the path: G:\Experiments\UA9\Data.

9.2. Files Data Format

Medipix

Time: local gateway writing time in dd/mm/yy hh:mm:ss

Frame: Medipix Matrix 256*256. The Medipix frame is made linear by rows. The array of 256*256 elements is so organized: the first 256 values of the array are the values of the X at Y=1, the next 256 values are the X values at Y=2 and so on up to Y=256.

aqnStamp: Machine timestamp in UTC

GEM1 and GEM2

Time: local gateway writing time in dd/mm/yy hh:mm:ss
Current: current array (ICAT_A, IG1U_A, IG1D_A, IG2U_A, IG2D_A, IG3U_A, IG3D_A, IPAD_A)
Frequency: Occurrences matrix organized as follows:
First 8 values in array are X values for Y = 1
Next 8 values in array are X values for Y = 2
and so on (until Y =16).
aqnStamp: Machine timestamp in UTC

Scintillation counters

The Scintillation counters acquisition frequency Fs is normally set at 50 Hz. The scintillation counters column contains the 50 samples array related to 1 s buffer acquisition. The column aqnStamp contains the timestamps array related to each sample. In particular:

Time: local gateway buffer writing time in dd/mm/yy hh:mm:ss
QD2Scintillator: samples array of the horizontal QD2 scintillator located upstream of the QD.52110
QD4Scintillator: samples array of the QD4 horizontal scintillator located upstream of the QD.52110
XRP2_1Scintillator: samples array of the XRP2_1 horizontal scintillator located upstream of the Tank
TEC2Scintillator: samples array of the TEC2 horizontal scintillator located upstream the Tank
Photomultiplier2: samples array of the Photomultiplier2 located inside the TAC
aqnStamp: timestamps array related
Photomultiplier1: samples array of the Photomultiplier1 located on the Si linear axis
QD3AndQD4Sum: samples array of the coincidences between QD3 & QD4
PhotomultiplierAndSum: samples array of the coincidences between Photomultiplier 1 & Photomultiplier 2
TEC3AndTEC4Sum: samples array of the coincidences between TEC3 & TEC4
TEC3Scintillator: samples array of the TEC3 vertical scintillator located downstream the Tank
QD1AndQD2Sum: samples array of the coincidences between QD1 & QD2
QD3Scintillator: samples array of the QD3 vertical scintillator located upstream the QD.52110
QD1Scintillator: samples array of the QD1 vertical scintillator located upstream the QD.52110
TEC4Scintillator: samples array of the TEC4 vertical scintillator located downstream the tank
TEC2AndXRP2_1Sum: samples array of the coincidences between TEC2 & XRP2_1

Positions A

The correspondence between axis number and motorization axis is specified in the following table:

Axis	Motorization	Switch Out position	LVDT measurement range
Axis 1	Cr1 CERN Goniometer 1- Linear Axis	Out of the beam (0 mm)	0 – 87.8 mm
Axis 2	Cr1 CERN Goniometer 1- Angular Axis	–6514 μrad	–6514 – 7890 μrad
Axis 3	Cr2 CERN Goniometer 2- Linear Axis	Out of the beam (0 mm)	0 – 88.8 mm
Axis 4	Cr2 CERN Goniometer 2- Angular Axis	–6940 μrad	–6940 – 7330 μrad
Axis 5	Si Linear Detector (photomultiplier 1)	Out of the beam (0 mm)	0 – 54.48 mm

Positions B

The correspondence between axes number and motorization axes is specified in the following table:

Axis	Motorization	Switch Out position	LVDT measurement range
Axis 1	Sc Scatter	Out of the beam (0 mm)	0 – 69.2 mm

Axis 2	IHEP goniometer axis 1	Out of the beam (0 mm)	To come
Axis 3	IHEP goniometer axis 2	Out of the beam (0 mm)	To come
Axis 4	Roman Pot 1 – Horizontal 1	Out of the beam (0 mm)	0 – 35.6 mm
Axis 5	Roman Pot 1 – Horizontal 2	Out of the beam (0 mm)	0 – 41.8 mm

Positions C

The correspondence between axes number and motorization axes is specified in the following table:

Axis	Motorization	Switch Out position	LVDT measurement range
Axis 1	Roman Pot 2 – Horizontal 1	Out of the beam (0 mm)	To come
Axis 2	Roman Pot 2 – Horizontal 2	Out of the beam (0 mm)	To come
Axis 3	Roman Pot 2 – Vertical 1	Out of the beam (0 mm)	To come
Axis 4	Roman Pot 2 – Vertical 2	Out of the beam (0 mm)	To come

TAC_position

The TAC position data are acquired at 1Hz. On the TAL is installed the photomultiplier 2. The data format is as follows:

Time: local gateway buffer writing time in d/m/y h/m/s
position: TAC position in mm. The displacement range is 0 - 72 mm.
switchin: positioned at 72 mm.
acqStamp: Machine timestamp in UTC
switchout: switch in position out of the beam (0 mm).

LSS5 Collimator positions

The data acquisition frequency is typical 1 Hz.

Time: local gateway buffer writing time in d/m/y h/m/s
switchAnticollUp: switch anticollision upstream between the two collimator jaws
switchRightDwstIn: switch in axis right downstream
switchLeftUpstOut: switch out axis left upstream
measuredAbsRightDownstream :position of the collimator axis right downstream (0 – 30 mm)
switchRightUpstIn: switch in axis right upstream
measuredAbsLeftUpstream: position of the collimator axis left upstream (0 – 30 mm)
measuredAbsRightUpstream: position of the collimator axis right upstream (0 – 30 mm)
switchLeftUpstIn: switch in axis left upstream
measuredAbsLeftDownstream: position of the collimator axis left downstream (0 – 30 mm)
measuredAbsGapDownstream: position of the collimator gap downstream (0 – 50 mm)
switchLeftDwstIn: switch in axis left downstream
switchAnticollDown: switch anticollision downstream between the two collimator jaws
switchRightDwstOut: switch out axis right downstream
switchLeftDwstOut: switch out axis left downstream
switchRightUpstOut: switch out axis right upstream
measuredAbsGapUpstream: position of the collimator gap upstream (0 50 mm)